Multi-criteria optimization of an earth-air heat exchanger for different French climates

Mathias Cuny, Arnaud Lapertot, Jian Lin, B. Kadoch, Olivier Le Métayer

Multi-criteria optimization of an earth-air heat exchanger for different French climates.

Mathias Cuny[a], Arnaud Lapertot[a], Jian Lin[b], Benjamin Kadoch[a,*], Olivier Le Metayer[a]

[a] *Aix Marseille Université, CNRS, IUSTI UMR 7343, 13453 Marseille, France.*
[b] *ICube UMR 7357, CNRS, IUT Robert Schuman, 72 Route du Rhin, 67411 Illkirch-Graffenstaden, France.*

Abstract

The Earth-Air Heat Exchanger (EAHE) is a system for cooling or preheating the blown air into a building. A modeling of this system is proposed from a model for the ground and a model for the exchanger. The results are in agreement between the outside air temperature of the numerical model and the experimental temperature measurements. A sensitivity analysis with factorial plans is carried out to determine the most impactful parameters, taking into account two energy criteria and one economic criterion. The results show that tube radius, tube length, air velocity, burial depth and soil nature are the most impactful parameters. A multi-criteria optimization study with genetic algorithms is then performed to determine the Pareto front. The criteria do not evolve in the same trend because when the cost of the energy recovered decreases, the coefficient of performance and the EAHE efficiency will deteriorate, and reciprocally. Finally, a multiple-criteria decision-making is carried out using the TOPSIS method to provide the optimal pipe configuration. The optimal solution provides a large tube length, an intermediate burial depth, and a small air velocity and tube radius. The EAHE can achieve strong energy performance in any French climate.

Keywords: earth-air heat exchanger, multiple-criteria decision-making, optimization multi-criteria, renewable energy, sensitivity analysis.

*Corresponding author
Email address: benjamin.kadoch@univ-amu.fr (Benjamin Kadoch)

1. Introduction

The residential sector accounts for 40 % of total energy consumption in developed countries [1]. To fight global warming, one of the European Union's strategies is to reduce energy consumption in buildings [2]. New regulations impose thermally insulated buildings using renewable energy systems and high-efficiency energy systems. In this context, ventilation heating systems are favored. For example, in Europe, heating, ventilation and air conditioning (HVAC) accounts for 68 % of the energy consumed in the residential sector [1].

The earth-air heat exchangers (EAHE) are renewable energy systems using ground temperature to preheat or cool the building. This system also allows the ventilation of the exhaust air of a building and the injection of renewed air from outside. The EAHE can improve the performance of a controlled mechanical ventilation for the heating system. The global energy performance of the system is thus improved by 29 % in winter and between 36 % and 46 % in summer [3]. In addition, the EAHE are very well suited to provide air ventilated at comfort temperature during the summer [4]. Such energy system is particularly suitable for contrasting climates, either for preheating [5], or for cooling [6]. This energy system is also suitable for temperate climates such as [7], [8] and [9]. The use of an EAHE and its energy performance are highly dependent on climatic conditions [10]. The first objective is to investigate if this system can be applied to temperate climates such as France. The soil type also allows improving the performance of the system. Indeed, the thermal performance can reach 15.9 % with a soil composed of sand [7]. Combined with a dual-flow controlled mechanical ventilation, the system's coefficient of performance (COP) is defined by the ratio between the heating capacity and the system consumption power and the COP can reach 16.3 [5].

The second objective is to apply a methodology of sensitivity analysis, multi-criteria optimization and multi-criteria decision-making. The aim is to determine the optimal design parameters. Sensitivity analysis quantifies the impact of parameter variation on defined criteria and makes it possible to classify the influence of the parameters. This method can be used to selected main pa-

rameters. This EAHE energy system can involve a large number of parameters and the sensitivity analysis could be used to reduce the number of parameters retained for the optimisation process [11]. Moreover, a multi-criteria optimization study is carried out with the main parameters. The aim is to determine the optimal design parameters that gives maximum performance and minimum cost. Indeed, the energy system must be optimized to be efficient and cheap. The main design parameters of an earth-air heat exchanger are: the material, diameter and length of the tube, the air flow velocity and the burial depth of the tube [12]. Concerning the COP of an EAHE, it can be optimal for a given length. Indeed, the difference between the air temperature flowing through the EAHE and the ground temperature decreases but pressure losses increase [13]. It is therefore not necessary to use exchangers of large length.

The third objective is to apply this energy system and this methodology for different French climates. Five French climatic zones are studied (H1a, H1b, H2b, H2c, H3), as illustrated in figure 1. Each climate is composed of its own specificity. Indeed, France is surrounded by a continental

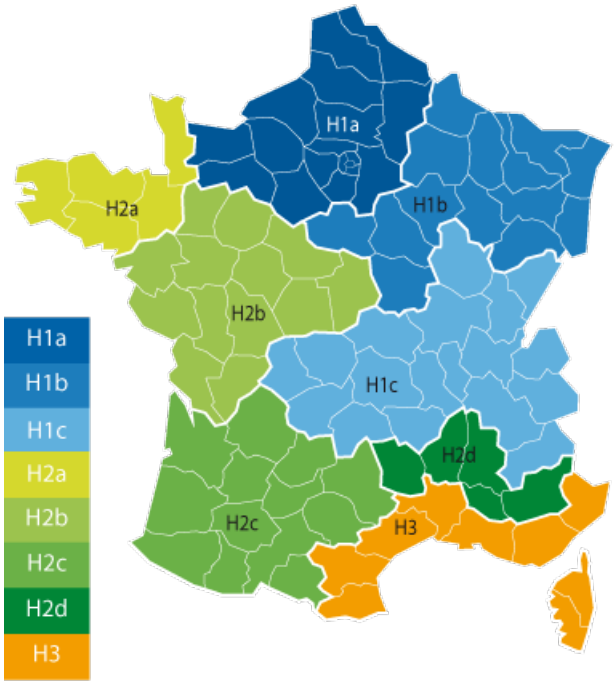

Figure 1: French climatic zones [14].

climate in the east, an oceanic climate in the west and north, and a Mediterranean climate in the south. Some French regions is constituted by a mountain climate due to the Pyrenees, the Alps, the Massif Central and the Vosges. Indeed, the continental climate is the most contrasting climate because it is characterized by a cold winter and a hot summer. Thus, the oceanic climate is influenced by the marine currents of the Atlantic Ocean, which provides a mild winter and a cool summer. Afterwards, the Mediterranean climate is composed of a hot and a dry summer and a mild winter. This climate has a lot of sunshine and wind. Then, the mountain climate is constituted by a mild and short summer, and a long and very cold winter. The difference between the climatic zones is based on meteorological data. Indeed, the outside air temperature and coefficients used to model the ground temperature are specific to each zone. Figure 2 shows the evolution of the outdoor air temperature for the different climatic zones in France [15]. Zone H3 has a stronger average temperature and a smaller temperature amplitude than the other zones. In addition, the H1b and H2b zones can have a very low air temperature in winter. Finally, zone H2c gives the most contrasted climate since the lowest and highest temperature are obtained for winter and summer, respectively. Indeed, the H1a and H2b zones have an oceanic and continental climate. The H1b and H2c zones not only have a continental climate but also a mountain climate. Zone H3 has a predominantly Mediterranean climate and a bit of mountain climate.

In this article, a multi-criteria optimization methodology is performed for different French climates. In section 2, the energy system and the different methods used will be described. Indeed, the EAHE is implemented from two distinct models. The first one simulates the thermal behaviour of the ground by computing the ground temperature, which is a function of depth and time. The second one models the air temperature between the inlet and the outlet of the EAHE. This annual dynamic modeling includes also the calculation of the power required by the fan to impose an air velocity. The experimental measurements and the numerical estimates of the outlet air temperature are compared in order to validate the model. In this study, several geometric parameters and the criteria are taken into account: two energy criteria (the EAHE efficiency and the COP) and an

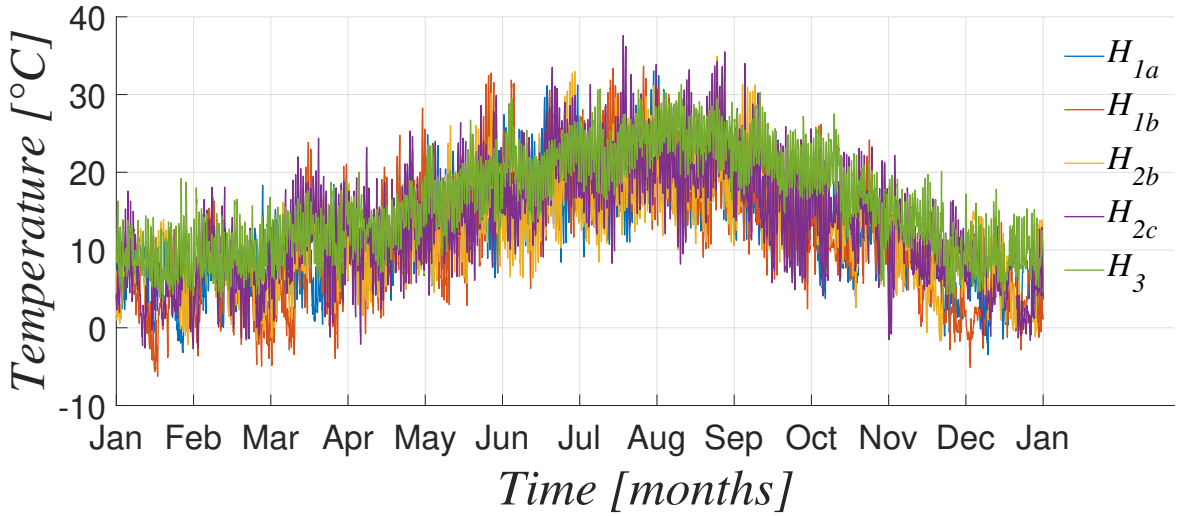

Figure 2: Temporal evolution of the outside air temperature for zone H1a (blue curve), zone H1b (red curve), zone H2b (orange curve), zone H2c (purple curve) and zone H3 (green curve) [15].

economic criterion (the cost of the energy recovered). Section 3 describes the results obtained by the sensitivity analysis, multi-criteria optimization and multi-criteria decision-making methods. Indeed, a sensitivity analysis is carried out to find the most impactful variables. Then, the design parameters are optimized according to the criteria to find the set of solutions that minimize the cost of the energy recovered, and maximize the EAHE efficiency and the COP. Finally, the optimal system pipe configuration is provided for five climatic zones studied (H1a, H1b, H2b, H2c, H3).

2. Modeling description and Methods

2.1. Modeling description

The models used for the EAHE system is based on studies [9] and [13]. The energy system is described in this subsection.

2.1.1. Description of the global system

The EAHE is composed of a pipe buried in the ground at a depth z. The tube is characterized by: a length L, an inner radius r and a thickness e. The air velocity v_{air} flowing through the EAHE is imposed by a fan located at its outlet (figure 3). The EAHE is the area of thermal contact between

two different sources: the air flowing through the tube, the soil surrounding the tube. In winter, the ground temperature is warmer than the outside air temperature. The air flowing through the EAHE heats up thanks to the warmth of the soil. The outlet air is warmer than the inlet air of the EAHE. In summer, the opposite phenomenon occurs and the outlet air is colder than the inlet air.

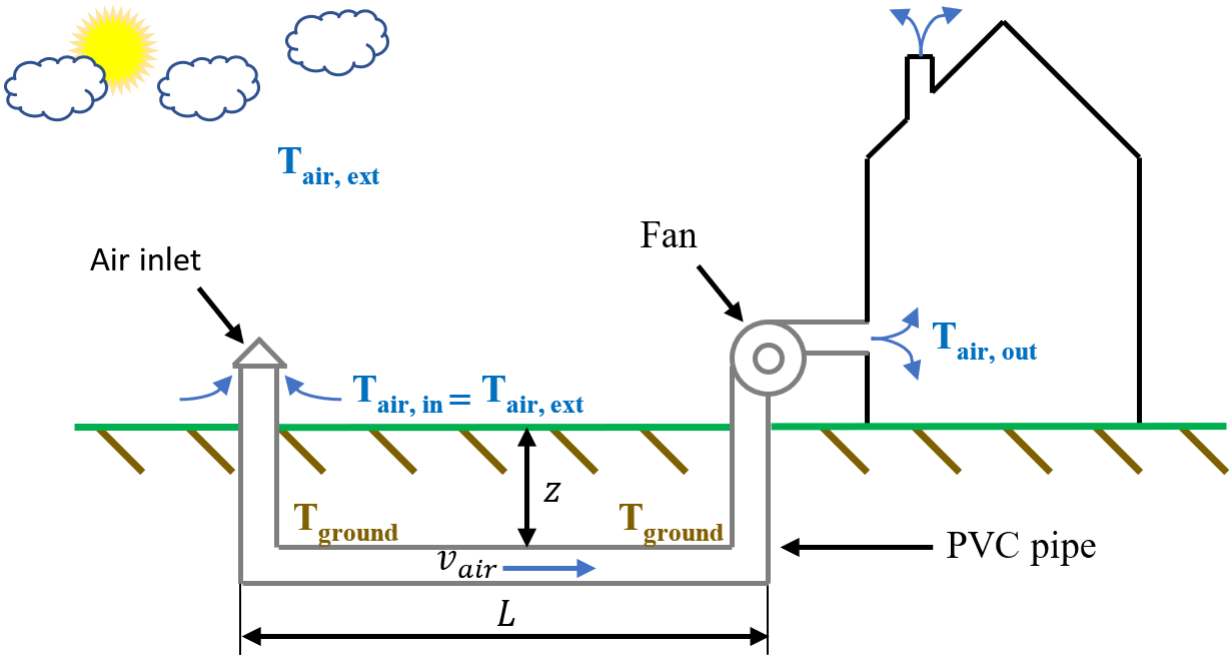

Figure 3: Structure of the ventilation system integrated into the building.

The EAHE is illustrated by a tube and the ground by a volume. The inlet air temperature of the tube $T_{air,\,in}$ corresponds to the outside air temperature $T_{air,\,ext}$. This temperature is easily measurable from hourly meteorological databases. However, the ground temperature at the soil-tube interface is difficult to obtain because the installation of a measuring device at the burial depth of the tube is problematic. In addition, these measurements are only valid for a single EAHE configuration. In this context, a system modeling is necessary. The hypothesis used for the EAHE model is taken from [9] and [13]:

1. a one-dimensional problem is considered;
2. the soil is considered as a homogeneous and isotropic medium;
3. the air and ground thermophysical properties are constant and independent of temperature.

The system is divided into one model for the ground and one for the EAHE.

2.1.2. The soil thermal model

The soil thermal model provides the ground temperature for any depth and at any time without taking into account the EAHE operation. The effects of mass and heat transfer are considered negligible due to small differences in ground temperatures [16]. The soil is considered as a semi-infinite homogeneous medium with constant thermophysical properties: thermal conductivity λ_{ground}, density ρ_{ground} and mass thermal capacity $c_{p_{ground}}$ [9]. In this study, the soil thermal model takes only into account thermal conduction.

Considering these hypotheses, the propagation of a sinusoidal temperature signal in a semi-infinite medium has an analytical solution [17]. In the investigated case, the sinusoidal temperature is the outside air temperature, it is written as follows:

$$T_{air,\,ext} = T_{mean} + \sum_{i=1}^{i=3} [T_i \ \sin(\omega_i t - \phi_i)] \tag{1}$$

with T_{mean} the average temperature over the tube, T_i the amplitude temperature, ω_i frequency oscillations, ϕ_i the phase shift. The oscillations consider an annual frequency ω_1, a monthly frequency ω_2 and a daily frequency ω_3 to take into account the annual, monthly and daily meteorological fluctuations. The amplitudes and the frequency are determined by the least square's method applied to meteorological data. The values of the amplitude and the phase shift are given in table 1. These values depend only on climatic zones. By applying this signal to the surface of a semi-infinite medium, the ground temperature is therefore given by:

$$T_{ground}(t,z) = T_{mean} + \sum_{i=1}^{i=3} T_i \ \exp\left(-z\sqrt{\frac{\omega_i}{2\,\alpha_{ground}}}\right) * \sin\left(\omega_i t - \phi_i - z\sqrt{\frac{\omega_i}{2\,\alpha_{ground}}}\right) \tag{2}$$

Zone	T_{mean}	T_1	T_2	T_3	ω_1	ω_2	ω_3	ϕ_1	ϕ_2	ϕ_3
Unit	$°C$	$°C$	$°C$	$°C$	s^{-1}	s^{-1}	s^{-1}	$-$	$-$	$-$
					$*10^{-7}$	$*10^{-6}$	$*10^{-5}$			
$H1a$	12.1	7.19	0.38	3.04	1.99	2.02	7.27	10.7	3.53	10.2
$H1b$	11.8	8.44	−0.80	3.34	1.99	2.02	7.27	10.7	3.53	10.4
$H2b$	12.3	6.61	−0.54	3.35	1.99	2.02	7.27	10.6	3.94	10.3
$H2c$	13.5	7.68	−0.61	4.13	1.99	2.02	7.27	10.6	4.77	10.2
$H3$	16.0	8.01	−0.34	2.89	1.99	2.02	7.27	10.5	−0.62	10.5

Table 1: Amplitude, frequency and phase shift values for the different French climates.

with α_{ground} the thermal diffusivity of the ground, which is defined by:

$$\alpha_{ground} = \frac{\lambda_{ground}}{\rho_{ground} * c_{p_{ground}}} \tag{3}$$

2.1.3. The EAHE model

The EAHE modeling gives the outlet air temperature. The air flowing through the EAHE is defined by a mass flow rate $\dot{m}_{air}$ and a constant mass heat capacity $c_{p_{air}}$. Depending on the direction of air flow, the tube is decomposed into several cylinders with the same length Δx (figure 4). For each cylinder, the air and ground temperatures are considered uniform. The power balance is written by:

$$\dot{m}_{air}\ c_{p_{air}} * \frac{dT_e}{dx} = UA_{air-tube} * (T_{ground} - T_e) \tag{4}$$

The mass of the tube is negligible compared to the mass of the ground. Consequently, the tube is characterized by its thermal conductance $UA_{air-tube}$. This variable is defined by:

$$\frac{1}{UA_{air-tube}} = \frac{1}{h_c * (2\pi r\ \Delta x)} + \frac{1}{2\pi r\ \Delta x\ \lambda_{tube}} * \ln\left(\frac{r+e}{r}\right) \tag{5}$$

where λ_{tube} is the thermal conductivity of the tube and h_c is the convective exchange coefficient

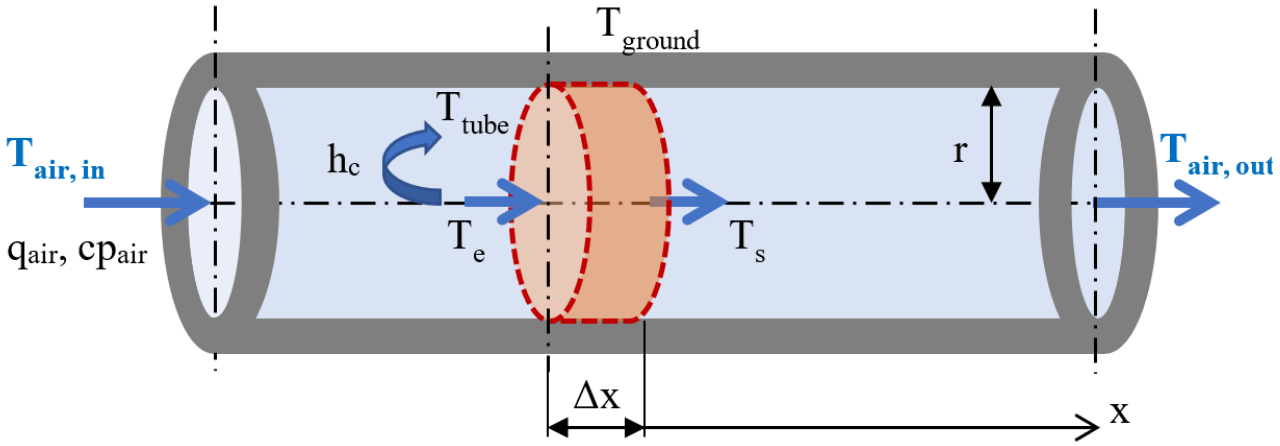

Figure 4: Schematization of the mesh size of an EAHE.

between the air and the tube. h_c is computed using formulations in forced convection [18] and it is written by:

$$h_c = 0.036 \, \frac{\lambda_{air}}{2r} * Re^{0.8} \, Pr^{\frac{1}{3}} * \left(\frac{2r}{\Delta x} \right)^{0.055} \tag{6}$$

with

$$\begin{cases} Re &= \dfrac{\rho_{air} \, v_{air} \, 2r}{\mu_{air}} \\ Pr &= \dfrac{\mu_{air} \, c_{p_{air}}}{\lambda_{air}} \end{cases}$$

the Reynolds number and the Prandtl number. μ_{air} is the air dynamic viscosity and λ_{air} is the air thermal conductivity.

At each time step, the outlet air temperature T_s is considered as the new inlet air temperature T_e for the following cylinder. The electrical power consumed by the fan at the output of the EAHE is defined by:

$$P_{fan} = \frac{1}{\eta_{fan}} \, \frac{\dot{m}_{air}}{\rho_{air}} \, \Delta p \tag{7}$$

with η_{fan} the electromechanical efficiency of the fan. Pressure losses of the system Δp are calculated

from [13] and are described by:

$$\Delta p = \left[f \, \frac{L}{2r} + 2 * 1.3 \right] \, \rho_{air} \, \frac{v_{air}^2}{2} \tag{8}$$

where the regular pressure losses coefficient f is defined by:

$$f = (1.82 \, \log(Re) - 1.6)^{-2} \tag{9}$$

2.1.4. Validation

The results from the EAHE model proposed in this study are compared to the experimental data of an EAHE installed on the IUT Robert Schuman geothermal platform (University of Strasbourg), including the meteorological data [8]. The procedure of model identification and boundary conditions are explains and details in [7].

The experimental EAHE is buried at 1.03 m in a multilayer soil: 10 cm of plant material, 60 cm of natural backfill and 50 cm of sand surrounding the tube. In addition, the EAHE is composed of a tube with a length and diameter equal to 17.5 m and 20 cm, respectively. Concerning the operating mode of the experimental measurements, the fan extracts the outside air at a speed of $0.51 \pm 0.02 \; m.s^{-1}$ at the tube outlet. Outside and outlet air temperatures are measured every 20 minutes with sensors PT100 with a accuracy of $\pm \, 0.1°C$. The geothermal platform is schematized by the figure 5.

Equations 2 and 4 are solved numerically at each time step during a full year using Runge-Kutta algorithm 4^{th} order with OpenModelica software [19]. In this study, the time step is 10 minutes and the hourly meteorological data are linearly interpolated. Figure 6 shows the evolution of the output air temperatures obtained from experimental data $T_{air\ out}^{exp}$ and the numerical model $T_{air\ out}^{num}$. Thermal behaviour of the EAHE model is similar to the measurements. The relative average error over the full year is 5.7 %. The modelled data are in good agreement with the experimental data.

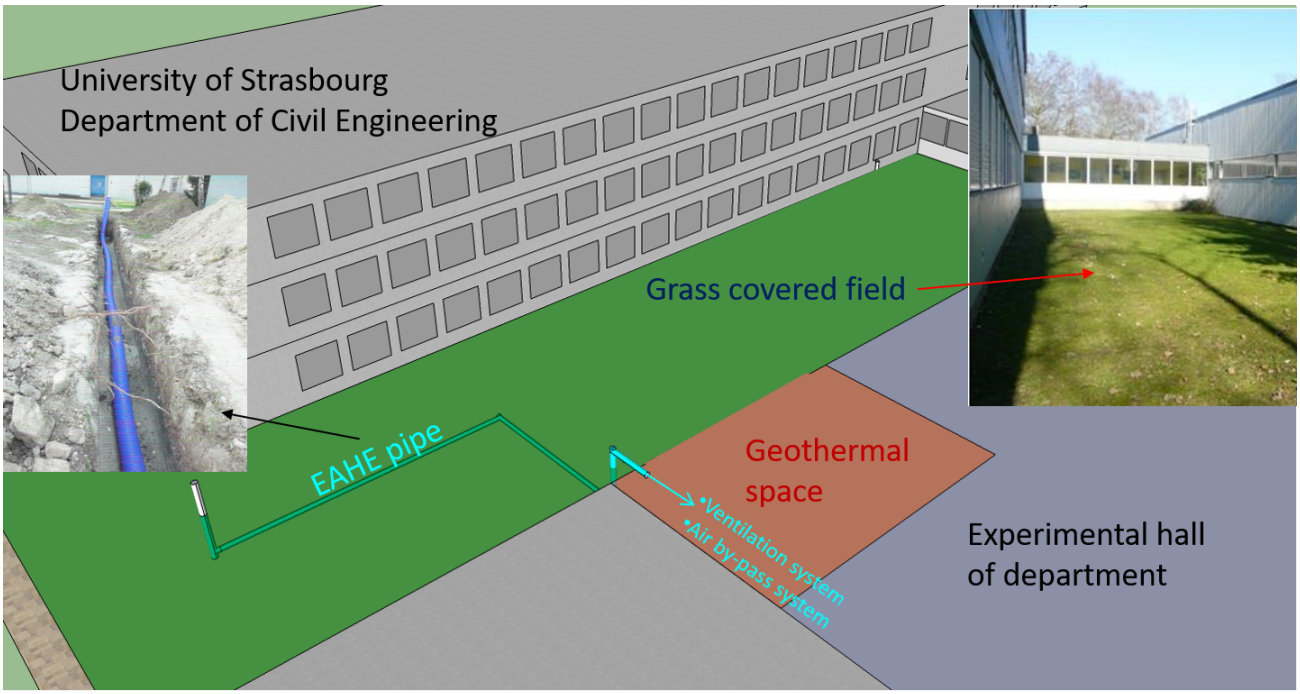

Figure 5: Schematization of the EAHE installed on the IUT Robert Schuman geothermal platform.

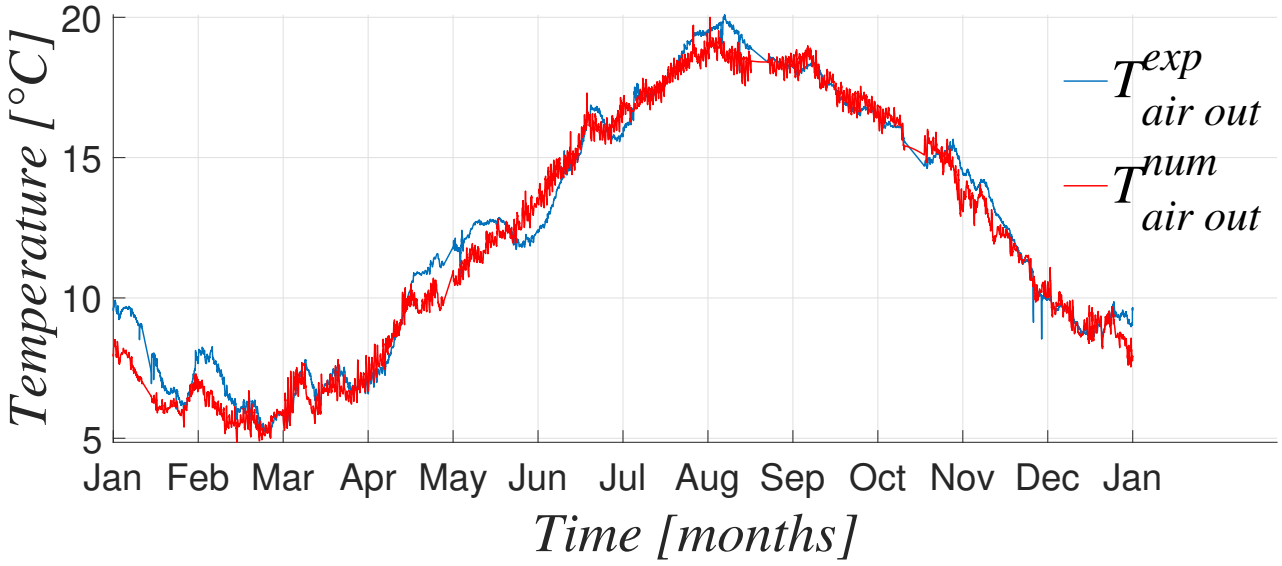

Figure 6: Outlet air temperature of the EAHE from the experimental data (in blue) and from the numerical modeling (in red).

2.2. Methods

The methods used for sensitivity analysis, multi-criteria optimization and multi-criteria decision-making is defined in this subsection.

2.2.1. Definition of variables and criteria

The tube parameters are characterized by a: radius r, length L, thickness e, rugosity ϵ_{tube}, thermal conductivity λ_{tube}, mass thermal capacity at constant pressure c_{tube} and density ρ_{tube}. Burial depth z, air velocity v_{air}, ground thermal conductivity λ_{ground}, mass thermal capacity at constant pressure of the ground $c_{p_{ground}}$ and ground density ρ_{ground} are also studied. Finally, the fan efficiency η_{fan} and the electricity price $price_{electricity}$ are taken into account. Parameters considered are summarized in table 2. The reference value corresponds to the experimental data.

Parameters	References	Units
r	0.1	m
L	17.5	m
e	0.005	m
ϵ_{tube}	0.015	mm
z	1.03	m
v_{air}	1.0	$m.s^{-1}$
λ_{tube}	0.6	$W.m.K^{-1}$
c_{tube} ρ_{tube}	2097600	$J.m^{-3}.K^{-1}$
λ_{ground}	2.7	$W.m.K^{-1}$
$c_{p_{ground}}$ ρ_{ground}	1210000	$J.m^{-3}.K^{-1}$
η_{fan}	0.63	$-$
$price_{electricity}$	0.12	€$/kWh$

Table 2: EAHE design parameters.

To quantify the EAHE performance, three criteria are defined: two energy criteria such as the average efficiency η_{EAHE} and the average coefficient of performance COP of the exchanger, and an economic criterion like the cost of the energy recovered (CER).

The average efficiency of an EAHE η_{EAHE} is the ratio between the energy recovered of the EAHE

and the recoverable energy over a one-year period T [13]:

$$\eta_{EAHE} = \frac{\int_0^T (T_{air,\,in} - T_{air,\,out})\ \mathrm{d}t}{\int_0^T (T_{air,\,in} - T_{ground})\ \mathrm{d}t} \tag{10}$$

The average COP is expressed by the ratio between the energy recovered and the energy consumed by the EAHE [13]:

$$COP = \dot{m}_{air}\ c_{p_{air}} * \frac{\int_0^T (T_{air,\,in} - T_{air,\,out})\ \mathrm{d}t}{\int_0^T (P_{fan})\ \mathrm{d}t} \tag{11}$$

The cost of the energy recovered CER is defined by the ratio between the total cost of an EAHE (installation cost, maintenance cost and operating cost) over its lifetime $N_{year} = 20$ years and the energy recovered by the EAHE [20].

$$CER = \frac{cost_{installation} + cost_{operation} + cost_{maintenance}}{N_{year}\ \dot{m}_{air}\ c_{p_{air}} * \int_0^T (T_{air,\,in} - T_{air,\,out})\ \mathrm{d}t} \tag{12}$$

The installation cost estimates the cost of workmanship such as earthworks and the cost of materials such as ventilators, air intake terminals and collectors. The installation cost is a function of tube length and burial depth. The operating cost is determined by the product of the electrical energy consumed by fans and the electricity prices. The maintenance cost quantifies the change of the filters three times per year.

2.2.2. Sensitivity analysis

The model validity and parameter sensitivity are studied in this section. This study consists in identifying and ranking the most impactful inputs, determining the non-impactful inputs and mapping the behaviour of the outputs in relation to the inputs [11]. To carry out this study, the factorial plan method is used as it can quantify the contribution of input parameters and their interactions. The two-level factorial plan requires 2^k calculations with k the number of inputs [21]. Therefore, factorial plans require more calculation than methods that vary one parameter at a

time, but they do provide information on the interactions between variables.

The factorial plan procedure is to approximate the objective function y by a linear system [20].

$$y = \gamma_0 + \sum_{i_1=1}^{k} \gamma_{i_1} \, X_{i_1} + \sum_{i_1=1}^{k} \sum_{i_1>i_2}^{k} \gamma_{i_1 \, i_2} \, X_{i_1 \, i_2} + ... + \gamma_{i_1 \, i_2 \, \ldots \, i_k} \, X_{i_1 \, i_2 \, \ldots \, i_k} \tag{13}$$

with γ_0 the mean of the objective function, γ_i the vector of the main effects of the parameters, $\gamma_{i_1 \, i_2}$ the vector of the interaction effects between parameters. X_i is composed of the normalized parameters vector.

$$\forall \, i \in [1, k], \; X_i = \frac{x_i - x_i^{ref}}{(x_i^{max} - x_i^{min})/2} \tag{14}$$

where x_i is characterized by the parameter value, x_i^{ref} the reference value, x_i^{max} the maximum value, x_i^{min} the minimum value. For the two-level factorial plan method, x_i is equal to its maximum or minimum value. Then the coefficients γ are obtained by solving the linear system 13. To obtain the contribution of the different parameters, the sum of squares must be defined.

$$\forall \, i \in [1, 2^k - 1], \; SS_i = 2^k \, \gamma_i^2 \tag{15}$$

Finally, the contribution percentage of each parameter and their interactions is thus determined by the following equation. PC which quantify the importance of parameters and couplings for each objective. The coupling corresponds to the interaction between parameters.

$$\forall \, i \in [1, 2^k - 1], \; PC_i = \frac{SS_i}{\sum_{i=1}^{k} SS_i} \tag{16}$$

In the investigated study, inputs correspond to variables or parameters ($k = 12$) and outputs referred to criteria or objectives. The most impactful parameters is determined using the factorial plan method [21].

2.2.3. Multi-criteria optimization

A multi-criteria optimization problem seeks to optimize several objective functions simultaneously. However, it does not provide an optimal solution because some objectives are not necessarily comparable. The works of Vilfredo Pareto [22] show that it is impossible to improve all criteria simultaneously, which means that the improvement of some objectives will necessarily degrade the other objectives. The result of the multi-objective optimization gives a set of solutions that have a good compromise for the different criteria, including the best solution of each criterion. These solutions come together on a curve called the Pareto front, which is composed of non-dominated solutions. A solution X is dominated by another solution Y if only, for any objective f_i, $f_i(X)$ is less than or equal to $f_i(Y)$ with at least one strict inequality. Many optimization methods exist as Nelder-Mead method, simplex method, particle swarm algorithms and genetic algorithms [23]. Genetic algorithms are suitable for constraints and multi-objectives problem. Genetic algorithms are probabilistic optimization methods based on the evolution of the species. They were developed originally by the works of John Holland [24]. Thanks to selection, crossing and mutation processes, individuals change over generations and the best performing species tend to survive in their natural environment.

In this case, genetic algorithms NSGA II [25] are performed with a percentage of mutation and crossing of 50 %, and with 100 individuals and 1000 generations, which corresponds to 100,000 evaluations per zone.

2.2.4. Multiple-criteria decision-making

Decision aid is a technique to choose on the best solution from a set of possible solutions. There are a number of multiple-criteria decision-making methods. The best known and used are the weighted sums and TOPSIS [26]. The Technique for Order Preference by Similarity to Ideal Solution TOPSIS is a decision aid technique developed originally in [26]. It consists in selecting the solution that has the shortest distance from the ideal solution.

In the investigated case, the best pipe configuration of the EAHE is selected using the TOPSIS

method. The ideal point is the maximum of the η_{EAHE} and the COP, and the minimum of the CER.

In this article, the optimization procedure is carried out in three steps. First, sensitivity analysis is used to determine the most impactful parameters in order to reduce the number of parameters. Then, multi-criteria optimization gives the set of solution that has a good compromise for the different criteria. Finally, the multi-criteria decision-making method selects one solution in the Pareto front. This selected solution is called the optimal solution.

3. Results and discussions

3.1. Sensitivity analysis

This section shows the results of the sensitivity study in order to select the most impactful parameters for multi-criteria optimization. The minimum x_{min} and maximum x_{max} limits for each variable are defined according to their reference values x_{ref} and a variable β varying from 5 % to 35 %:

$$\begin{cases} x_{min} = x_{ref} * (1 - \beta) \\ x_{max} = x_{ref} * (1 + \beta) \end{cases}$$

3.1.1. Parameter sensitivity

Figure 7 illustrates the contribution percentages PC. The first graph in figure 7 shows contribution percentages of the variables for the η_{EAHE}. Tube radius, tube length and air velocity are the three most impactful parameters because they correspond respectively to 53 %, 42 % and 2 % of the general variation of the η_{EAHE}. However, r, L and v_{air} have a small contribution for different β. Furthermore, ground thermal conductivity λ_{ground} has a percentage, which increases with β and reaches 3 %. Other parameters and couplings have no impact for the η_{EAHE}. The second graph in figure 7 shows the results for the COP. Tube radius is predominant for the COP and decreases

between 75 % and 60 % when β increases. Moreover, air velocity contributes 20 % of the general evolution of the COP. Similarly, parameter L and the coupling $r - v_{air}$ are small but increase with β, they exhibits 12 % and 2 %, respectively. Then, the burial depth has a small contribution, which is dependent on β. Finally, other variables have no impact for the COP. The graph in figure 7 exhibits the contribution percentages for the CER. Tube radius r is the dominant variable for the CER. This parameter decreases with β, because it goes from 70 % to 60 % when β increases. In addition, the contribution of air velocity and tube length are important independently of β. The influences of v_{air} and L are equal to 20 % and 6 %, respectively. Similarly, the parameter $\rho_{ground} * c_{p_{ground}}$ and the coupling between r and v_{air} have a low contribution percentage but they increase with β. The contribution of the other parameters is negligible for the CER.

3.1.2. Physical interpretation

In summary, the most impactful parameters are tube radius, tube length, air velocity, burial depth and soil nature for three criteria considered. The impact of each parameter on the objectives are explained by carrying out a physical interpretation.

Tube radius has an influence on the EAHE efficiency, on the coefficient of performance and on the cost of the energy recovered. Indeed, tube radius is correlated to the outlet air temperature of the EAHE (eq 10-12) and has an impact on the pressure drop and the fan power (eq 7-8). As a consequence, when r increases, Δp and $\Delta T = \| T_{air\ out} - T_{air\ in} \|$ decrease, so the heat exchanges are lower quality. Δp and ΔT decrease independently. Therefore, when r increases, the CER increases, the COP and η_{EAHE} decrease.

In addition, air velocity has a contribution to the three objectives because v_{air} is directly related to the air mass flow rate. Indeed, the fan power (eq. 7) and the power balance (equation 4) depend on the mass flow rate of air. Finally, the air velocity is correlated to the operating cost of the system which depends on the fan power. Therefore, when v_{air} increases, the heat exchanges between soil and air, Δp and $cost_{operation}$ increase. Thus when v_{air} increases, the CER increases, the η_{EAHE} and COP decrease.

Similarly, tube length has an influence on the criteria. Indeed, pressure drops (eq. 8) and the outlet air temperature of the EAHE depend on tube length. It affects also the installation cost which is also related to the installation cost of the system. When L increases, the ground-air heat exchanges, Δp and $cost_{installation}$ increase. Consequently, when L increases, the η_{EAHE} and the COP increases, the CER decreases.

Furthermore, burial depth z has an influence on the three objectives. According to the equation 2, the ground temperature depends on z and has a contribution on the outlet air temperature of the EAHE (eq. 4) and on the EAHE efficiency (eq. 10). Burial depth is also correlated to the installation cost of the system. So, when z increases, $cost_{installation}$ increases, and T_{ground}, $T_{air\ out}$ increase in winter and decrease in summer, so the heat exchanges are better. Therefore, when z increases, the COP increases, the CER and η_{EAHE} decrease.

Moreover, the soil thermophysical properties λ_{ground} and $\rho * c_{p_{ground}}$ have an impact on the η_{EAHE}, the COP and the CER. Indeed, the ground temperature is defined by a function of the ground thermal diffusivity (eq. 2). As previously for burial depth, the ground temperature is related to the outlet air temperature of the EAHE (eq. 4) and thus to the three objectives. When α_{ground} increases, the heat exchanges between the soil and the air are lower quality so the COP decreases and the CER and the η_{EAHE} increase.

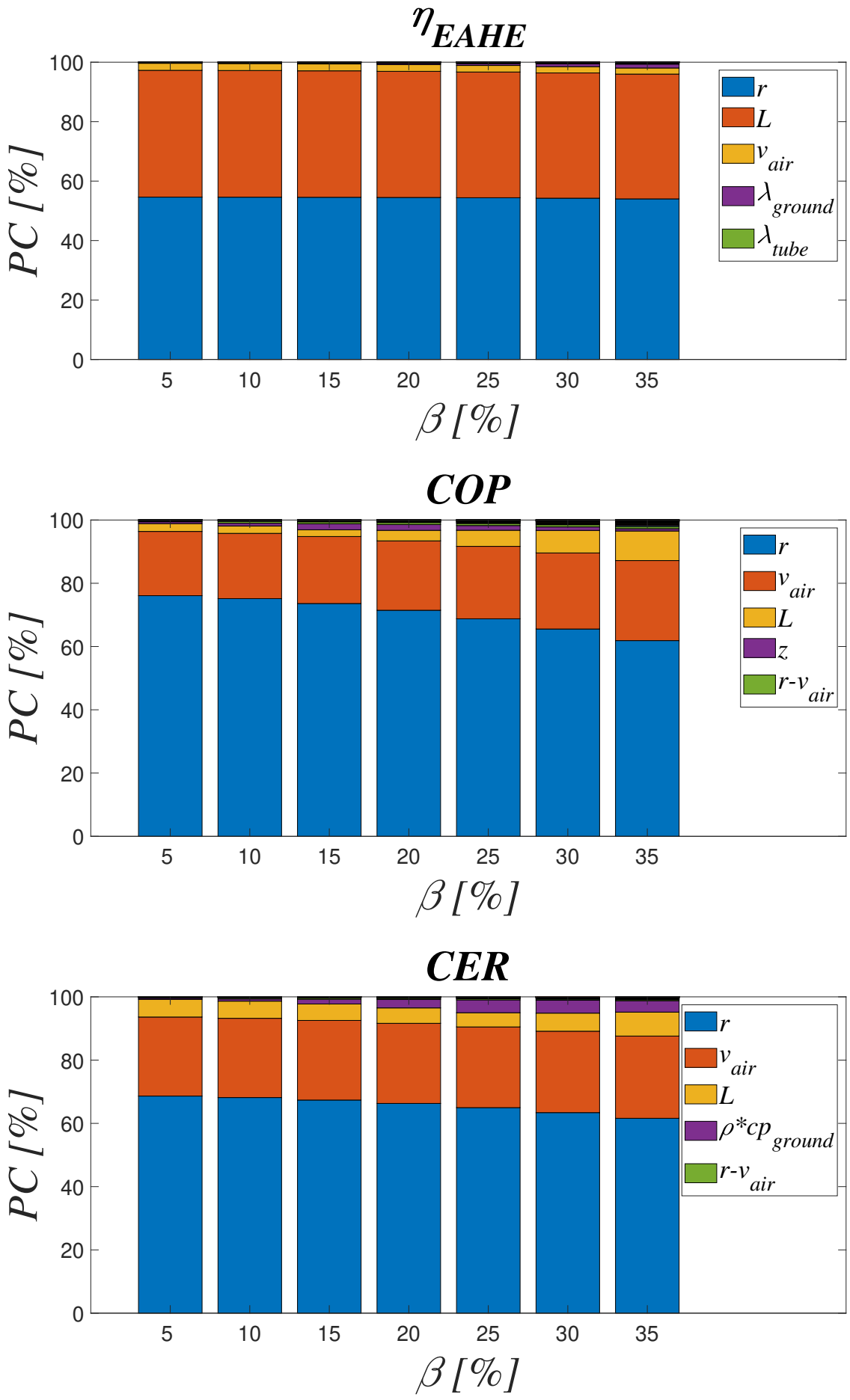

Figure 7: Percentage contribution of variables for the different objectives.

3.1.3. Choice of parameters for optimization

Based on the sensitivity study, the variables selected for the optimization of the EAHE are: tube radius r, tube length L, burial depth z, air velocity v_{air} and soil nature characterized by its thermal diffusivity α_{ground}. These parameters have a significant influence on the performance of an EAHE. The results allowed obtaining the same design parameters given by [12] and the soil nature provided by [27]. Other parameters are considered negligible. The reference values are used for these parameters for the rest of the study. In this case, the boundary values are summarized in table 3 and correspond to the design boundary values of an EAHE for a single-family house of 450 m^3 [12]. Air renewal in the house requires a minimum volume flow rate of 150 $m^3.h^{-1}$. A constraint on the volume flow rate at the outlet of the EAHE ensures this minimum air change.

Parameters	r	L	z	v_{air}	α_{ground}
Units	m	m	m	$m.s^{-1}$	$*10^{-6}\ m^2.s^{-1}$
Minimum	0.05	10.0	0.50	1.00	0.376
Maximum	0.50	100.0	5.00	10.0	0.970

Table 3: Range of values for the design parameters and for the nature of the soil characterized by its thermal diffusivity.

Three types of ground [9] are commonly present when installing an EAHE. These values are selected for the study, see table 4.

Soil nature	I_{ground}	λ_{ground}	$c_{p_{ground}}$	ρ_{ground}	α_{ground}
Units	$-$	$W.m^{-1}.K^{-1}$	$J.kg^{-1}.K^{-1}$	$kg.m^{-3}$	$*10^{-6}\ m^2.s^{-1}$
Clay	1	880	1.28	1500	0.970
Sandy-clay silt	2	1340	1.50	1800	0.622
Sand	3	1390	0.93	1780	0.376

Table 4: Thermophysical properties for the three types of soil.

3.2. Multi-criteria optimization

The selected parameters for optimization are: tube radius r, tube length L, burial depth z, air velocity v_{air} and three soil types characterized by the ground index I_{ground}. These variables vary

315 independently over the range shown in tables 3 and 4. This optimization procedure is carried out for each climatic zone with different boundary conditions [15]. The optimization results are described using two formats: Pareto front and mapping. Due to the large number of graphs generated, this section only presents the results for zone H1a. Other areas have the same trend.

320 Figure 8 illustrates the Pareto front, which is a function of each objective. The best solutions vary from 0.12 to 0.26 €/kWh for the CER, 2.9 to 14.8 for the COP and 0.90 to 0.98 for the η_{EAHE}. The criteria do not evolve in the same trend because if the cost of the energy recovered decreases, the coefficient of performance and the EAHE efficiency will deteriorate, and inversely. Figure 8a refers to the ground index. Two forms can be distinguished: blue points correspond 325 to a clayey-sand silt ($I_{ground} = 2$) and red points to sand ($I_{ground} = 3$). The CER is small with silty soil and the η_{EAHE} is strong with sand. The solutions obtained with clay soil are dominated, which is why no points are in figure. Figure 8b shows the best solutions are obtained for tube length varying from 90 to 100 meters. When the tube length increases, the CER and the COP decrease because pressure losses increase. Indeed, when L increases, the η_{EAHE} increases due to a 330 better heat exchange between the ground and the air. Figure 8c exhibits the Pareto front for tube radius between 0.12 and 0.20 meters. When tube radius increases, the COP, the CER and the η_{EAHE} decrease. Indeed, when r increases, the exchanges between soil and air are lower quality and pressure losses are smaller. Figure 8d shows the dominant solutions for air velocity varying from 0.6 to 1.6 $m.s^{-1}$. When air velocity increases, the COP and the CER decrease, and the 335 η_{EAHE} increases. The same observation is obtained for tube length. Figure 8e exhibits the good compromises for a burial depth ranging from 2.4 to 4 meters. The burial depth varies according to the type of soil: between 2.4 and 3.4 meters for the sand and 3 to 4 meters for the clay-sand silt. For any type of soil, the CER decreases for decreasing z, this result is consistent since the system cost depends on its depth.

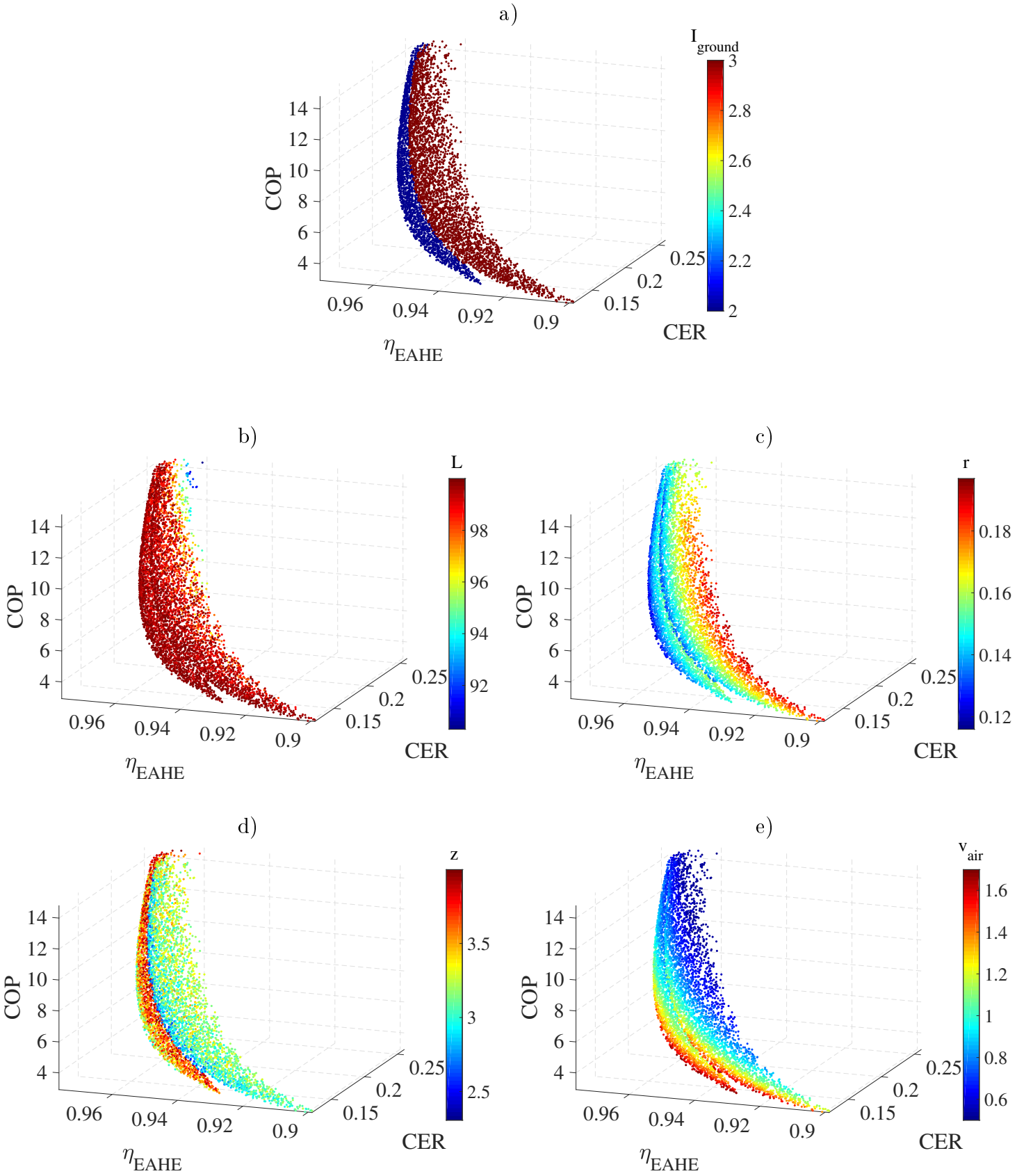

Figure 8: Pareto front for the different parameters.

Mapping allow exhibiting objectives according to parameters for all solutions obtained during the process. Each point corresponds to one simulation.

Figure 9 shows the EAHE efficiency as a function of air velocity v_{air} and tube length L (left), and as a function of tube radius r and soil index I_{ground} (right). The EAHE efficiency values are included between 0 and 0.98. The results show that the η_{EAHE} increases when L and I_{ground} increases, and when v_{air} and r decrease. The points on the Pareto front, illustrate by the pink dots, are located for a large length, small air velocity and tube radius, and for soil index $I_{ground} = 2,\ 3$. Figure 9 on the right shows that there is indeed no solution for a clay soil ($I_{ground} = 1$).

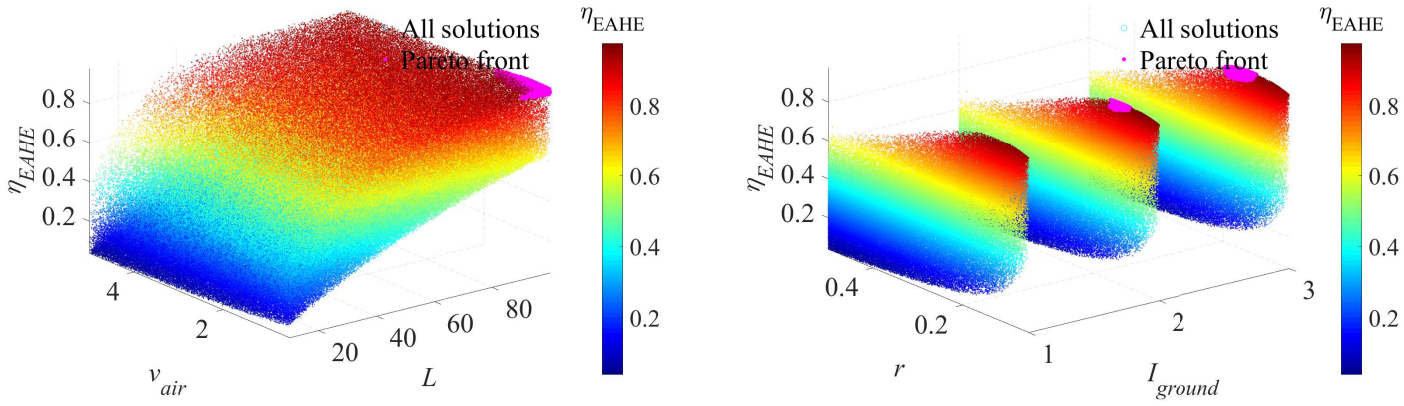

Figure 9: Evolution of the EAHE efficiency η_{EAHE} according to the air velocity and burial depth (left) and according to the tube radius and the ground index (right). The Pareto front is constituted by the pink dots.

Figure 10 shows the COP for burial depth z, air velocity v_{air} and for tube length L, tube radius r. The coefficient of performance values are between 0 and 14.8. The coefficient of performance increases when v_{air} and r decrease, and when z and L increase. In addition, the COP achieves an optimal value for a burial depth, an air velocity, a length and a radius equal to 2.3 m, 0.8 $m.s^{-1}$, 100 m, 0.1 m, respectively. The Pareto front is located for small air velocity and tube radius, intermediate burial depth and large length.

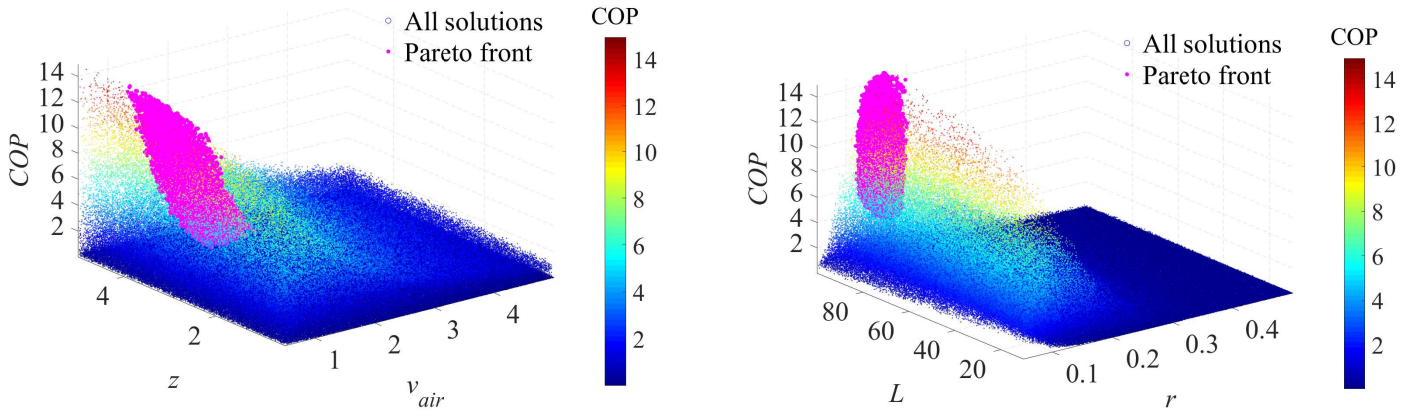

Figure 10: Evolution of the COP according to air velocity and burial depth (left) and according to the length and radius of the tube (right). The Pareto front is constituted by the pink dots.

Figure 11 illustrates the CER as a function of air velocity and tube radius. According to this figure, the cost of the energy recovered can vary between 0.12 and 2000 €/kWh. Moreover, air velocity and radius of the tube increases with the CER. Furthermore, the Pareto front is located for small values of v_{air} and r, for a large L and for an average burial depth (3 m). However, it was not possible to obtain solutions for a minimum air velocity and tube radius because they do not respect the minimum volume flow constraint: $q_{air} > 150\ m^3.h^{-1}$.

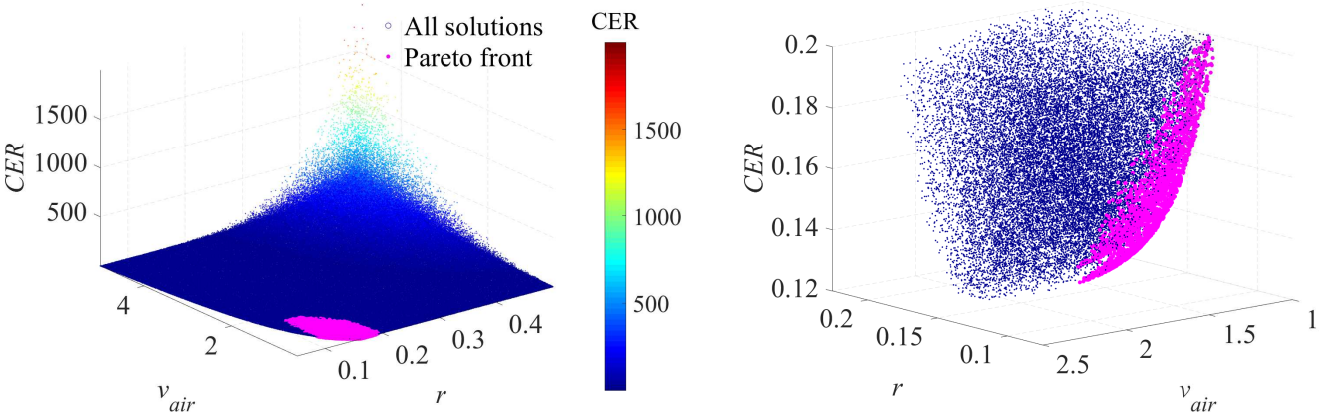

Figure 11: Evolution of the CER according to the air velocity and the tube radius (left). Zoom of the Pareto front (right). The Pareto front is constituted by the pink dots.

3.3. Multiple-criteria decision-making

The optimization method made possible to obtain the Pareto front. In order to install this system, it is essential to select a single solution for the optimal pipe configuration of the EAHE. For these reasons, decision aid methods are used.

Table 5 summarizes the best solutions for different French climates. The optimal values are between 0.17 and 0.23 €/kWh for the CER, 11.4 to 14.4 for the COP and between 0.96 and 0.97 for the η_{EAHE}. Furthermore, the ground index corresponds to sand ($I_{ground} = 3$). The value of parameters varies between 14 and 16 cm for r, from 97 to 98 meters for L, from 2.9 to 3.3 meters for z, from 0.7 to 0.8 $m.s^{-1}$ for v_{air}. As a result, the disparity on values is small.

The cost of the energy recovered is optimal when the total cost is minimal and when the energy recovered is maximum. Indeed, a small air velocity and a small burial depth will generate little cost. In addition, a large tube length and a small tube radius will increase the difference between the output and input air temperature of the EAHE. It is necessary to obtain the strongest possible temperature difference to maximize the energy recovered. Then, the EAHE efficiency is stronger when the outlet air temperature is very close to the ground temperature. The latter is obtained where the tube length is very large and the tube radius is small. Finally, the coefficient of performance is maximum when the energy recovered is maximum and when the energy consumed is minimal. For the same reasons, the energy recovered is maximum for a large tube length and a small tube radius. Moreover, a small air velocity will cause a minimal energy consumption.

The mean and the relative average error are defined by:

$$\bar{x} = \frac{1}{5} \sum_{Hi} x_{Hi} \qquad \sigma = \frac{|x_{Hi} - \bar{x}|}{\bar{x}} \tag{17}$$

with x_{Hi} the value of parameters or objectives for the climate zone Hi.

Therefore, to achieve optimal pipe configuration, the EAHE must be buried in sandy soil at a burial depth of 3.2 meters, a tube radius of about 15 cm and a tube length of 97 meters. The

/	Objectives				Variables			
Name	CER	COP	η_{EAHE}	I_{ground}	r	L	z	v_{air}
Units	€$/kWh$	$-$	$-$	$-$	m	m	m	$m.s^{-1}$
H1a	0.21	11.4	0.96	sand	0.15	96.9	2.91	0.72
H1b	0.17	13.4	0.96	sand	0.16	97.6	3.22	0.67
H2b	0.23	12.0	0.97	sand	0.14	97.5	3.26	0.71
H2c	0.20	14.4	0.97	sand	0.14	96.6	3.05	0.69
H3	0.19	11.8	0.96	sand	0.15	98.2	3.41	0.76
$\bar{x}$	0.20	12.6	0.96	/	0.15	97.4	3.17	0.71
σ [%]	8.0	8.3	0.3	/	4.3	0.5	4.8	3.4

Table 5: Results of the multi-criteria optimization methodology for different French climates.

air velocity should be fixed at 0.7 $m.s^{-1}$, which is equivalent to a volume flow of 175 $m^3.h^{-1}$; the minimum volume flow constraint is thus respected. The criteria values are 0.20 €$/kWh$, 12.6, 0.96 for the CER, the COP, the η_{EAHE}, respectively. The total cost of the system is about 11400 € over 20 years including 58 % for the installation cost, 36 % for the maintenance cost and 5 % for the operation cost. The energy recovered by the system is approximately 2920 kWh and the energy consumed by fans is around 240 kWh. The relative average error on the geometric parameters are less than 10 % so the EAHE can achieve strong energy performance in any French climate.

4. Conclusions

In this study, a methodology for optimizing the design parameters of an EAHE was carried out for different French climates. The proposed modeling of the system was divided into two models, one for soil and one for the EAHE. The model was validated using experimental measurements from the Robert Schuman Institute of Technology (University of Strasbourg). A sensitivity analysis was carried out on the design parameters of the EAHE according to two energy criteria (the average efficiency and the coefficient of performance) and an economic criterion (the cost of the energy recovered). The results show that tube radius, tube length, burial depth, ventilated air velocity and soil nature are the most impactful parameters. These ones were selected for multi-criteria optimization. Multi-criteria optimization was performed on the EAHE system. The criteria do

not evolve in the same trend. Indeed, if the cost of the energy recovered decreases, then the coefficient of performance and the EAHE efficiency will deteriorate, and inversely. Pareto front solutions give a small tube radius, a large length, an intermediate burial depth and a small air velocity. Finally, a multi-criteria decision-making method was applied to determine the optimal pipe configuration. The EAHE should be buried in a sandy ground, at a burial depth of 3.2 meters, a tube radius of 15 cm, a tube length of 97 meters, a ventilated air velocity of 0.7 $m.s^{-1}$. In this case, the value of objectives is 0.20 €/kWh, 12.6, 96.4 % for the CER, the COP, the η_{EAHE}, respectively. In addition, the values obtained are of the same order of magnitude for each climate zone. In complement to this study, it would be interesting to study the sensitivity and optimization of an EAHE associated with controlled mechanical ventilation with double flow and a building. This kind of system is able to renew air inside the home and could satisfy the demand for heating and cooling. Finally, this methodology can be applied for any climate. Similar results can be expected for comparable climates but the results will not necessarily be the same for contrasting climates.

Acknowledgement

The authors express their gratitude to M. Siroux and C. Fond for the use of experimental data from the geothermal platform of the University of Strasbourg.

References

[1] L. Pérez-Lombard, J. Ortiz, C. Pout, A review on buildings energy consumption information, Energy and Buildings 40 (2008) 394–398. doi:10.1016/j.enbuild.2007.03.007.

[2] The European Parliament and the Council of the European Union, Directive 2010/31/eu of the european parliament and of the council of 19 may 2010 on the energy performance of buildings, https://eur-lex.europa.eu/LexUriServ/LexUriServ.do?uri=OJ:L:2010:153:0013:0035:EN:PDF, accessed 21 November 2019 (2010).

[3] F. Ascione, D. D'Agostino, M. Concetta, F. Minichiello, Earth-to-air heat exchanger for nzeb in mediterranean climate, Renewable Energy 99 (2016) 553–563. doi:10.1016/j.renene.2016.07.025.

[4] T. M. Yusof, H. Ibrahim, W. H. Azmi, M. R. M. Rejab, Thermal analysis of earth-to-air heat exchanger using laboratory simulator, Applied Thermal Engineering 134 (2018) 130 – 140. doi:10.1016/j.applthermaleng.2018.01.124.

[5] H. Li, L. Ni, G. Liu, Z. Zhao, Y. Yao, Feasibility study on applications of an earth-air heat exchanger (eahe) for preheating fresh air in severe cold regions, Renewable Energy 133 (2018) 1268–1284. doi:10.1016/j.renene.2018.09.012.

[6] F. Fazlikhani, H. Goudarzi, E. Solgi, Numerical analysis of the efficiency of earth to air heat exchange systems in cold and hot-arid climates, Energy Conversion and Management 148 (2017) 78–89. doi:10.1016/j.enconman.2017.05.069.

[7] M. Cuny, J. Lin, M. Siroux, V. Magnenet, F. C., Influence of coating soil types on the energy of earth-air heat exchanger, Energy and Buildings 158 (2018) 1000 – 1012. doi:https://doi.org/10.1016/j.enbuild.2017.10.048.

[8] J. Lin, H. Nowamooz, S. Braymand, P. Wolff, C. Fond, Impact of soil moisture on the long-term energy performance of an earth-air heat exchanger system, Renewable Energy (2018) 0960–1481. doi:10.1016/j.renene.2018.06.106.

[9] S. Thiers, B. Peuportier, Thermal and environmental assessment of a passive building equipped with an earth-to-air heat exchanger in France, Solar Energy 82 (2008) 820–831. doi:10.1016/j.solener.2008.02.014.

[10] Z. Li, W. Zhu, T. Bai, M. Zheng, Experimental study of a ground sink direct cooling system in cold areas, Energy and Buildings 41 (2009) 1233–1237. doi:10.1016/j.enbuild.2009.07.020.

[11] A. Saltelli, M. Ratto, T. Andres, F. Campolongo, J. Cariboni, D. Gatelli, M. Saisana, S. Tarantola, Global Sensitivity Analysis. The Primer, Vol. 304, John Wiley & Sons, 2008. doi:10.1002/9780470725184.

[12] N. Bordoloi, A. Sharma, H. Nautiyal, V. Goel, An intense review on the latest advancements of earth air heat exchangers, Renewable and Sustainable Energy Reviews 89 (2018) 261–280. doi:10.1016/j.rser.2018.03.056.

[13] M. Benhammou, B. Draoui, Parametric study on thermal performance of earth-to-air heat exchanger used for cooling of buildings, Renewable and Sustainable Energy Reviews 44 (2015) 348–355. doi:10.1016/j.rser.2014.12.030.

[14] Les différentes zones climatiques françaises, https://neuf.cabinet-bedin.com/performances-energetiques, accessed 12 September 2019.

[15] Les données météorologiques RT 2012, https://www.rt-batiment.fr/batiments-neufs/reglementation-thermique-2012/donnees-meteorologiques.html, accessed 1 June 2019.

[16] C. Saix, J. Benet, G. Dellavalle, P. Jouanna, Physical Model for the Study of Mass and Energy Transfers in the Non-Saturated Layer of Soil Located Above a Solar Energy Storage Zone, 1984. doi:10.1007/978-94-009-6508-9_177.

[17] J. F. Sacadura, Initiation Aux Transferts Thermiques., Fourth Printing. Techniques et Documentation, 1973.

[18] M. Ozisik, Heat Transfer: A basic approach., McGraw-Hill, 1985.

[19] O. S. M. Consortium, Openmodelica, https://openmodelica.org, accessed 21 November 2019 (2019).

[20] S. Launay, B. Kadoch, O. Le Métayer, C. Parrado, Analysis strategy for multi-criteria optimization: Application to inter-seasonal solar heat storage for residential building needs, Energy 171 (2019) 419–439. doi:10.1016/j.energy.2018.12.181.

[21] D. C. Montgomery, Design and analysis of experiments, 8th Edition, John Wiley & Sons, 2013.

[22] M. Ehrgott, Multicriteria Optimization, Springer-Verlag, Berlin, Heidelberg, 2005.

[23] R. K. Arora, Optimization: Algorithms and applications, Hoboken : CRC Press, 2015. doi:10.1201/b18469.

[24] J. Holland, Adaptation In Natural And Artificial Systems, University of Michigan Press, 1975.

[25] K. Deb, A. Pratap, S. Agarwal, T. Meyarivan, A fast and elitist multiobjective genetic algorithm: NSGA-II, Evolutionary Computation, IEEE Transactions on 6 (2002) 182 – 197. doi:10.1109/4235.996017.

[26] G. H. Tzeng, J. J. Huang, Multiple attribute decision making: Methods and applications, CRC Press, Taylor and Francis Group, A Chapman & Hall Book, Boca Raton, 2011. doi:10.1201/b11032.

[27] E. Sipio, D. Bertermann, Factors influencing the thermal efficiency of horizontal ground heat exchangers, Energies 10 (2017) 1897. doi:10.3390/en10111897.